

Accepted Manuscript

Metal-Dependent Structural Variations Based on Mixed Ligands of 5-Hydroxy Isophthalic Acid and 1,3-Bis(imidazol-1-ylmethyl)benzene: Solvothermal Syntheses, Structural Characterizations, Luminescence and Magnetic Properties

Xiutang Zhang, Liming Fan, Weiliu Fan, Xian Zhao

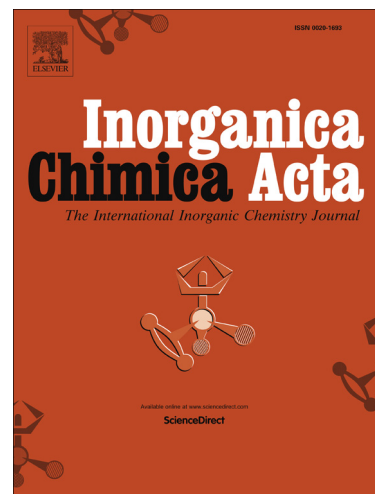
PII: S0020-1693(15)00527-7
DOI: <http://dx.doi.org/10.1016/j.ica.2015.10.033>
Reference: ICA 16743

To appear in: *Inorganica Chimica Acta*

Received Date: 27 May 2015
Revised Date: 4 October 2015
Accepted Date: 16 October 2015

Please cite this article as: X. Zhang, L. Fan, W. Fan, X. Zhao, Metal-Dependent Structural Variations Based on Mixed Ligands of 5-Hydroxy Isophthalic Acid and 1,3-Bis(imidazol-1-ylmethyl)benzene: Solvothermal Syntheses, Structural Characterizations, Luminescence and Magnetic Properties, *Inorganica Chimica Acta* (2015), doi: <http://dx.doi.org/10.1016/j.ica.2015.10.033>

This is a PDF file of an unedited manuscript that has been accepted for publication. As a service to our customers we are providing this early version of the manuscript. The manuscript will undergo copyediting, typesetting, and review of the resulting proof before it is published in its final form. Please note that during the production process errors may be discovered which could affect the content, and all legal disclaimers that apply to the journal pertain.



For Table of Contents Use Only
Table of Contents Graphic and Synopsis

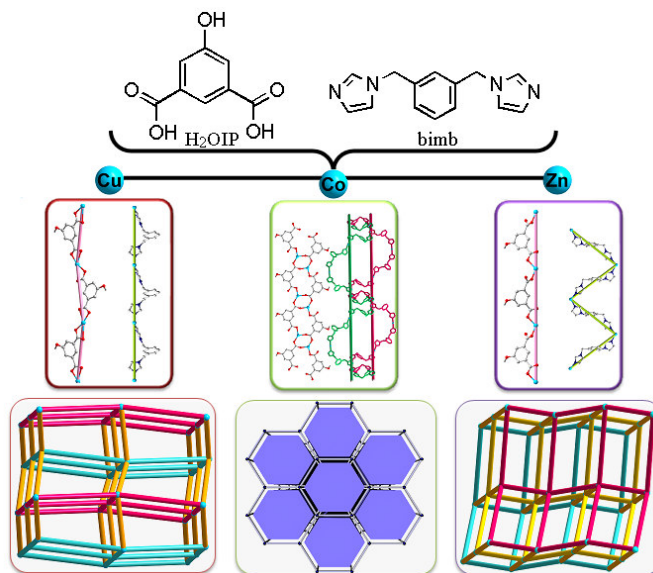
**Metal-Dependent Structural Variations Based on Mixed Ligands of 5-Hydroxy
Isophthalic Acid and 1,3-Bis(imidazol-1-ylmethyl)benzene: Solvothermal Syntheses,
Structural Characterizations, Luminescence and Magnetic Properties**

Xiutang Zhang (X. Zhang), Liming Fan (L. Fan), Weiliu Fan (W. Fan), and Xian Zhao (X. Zhao)

Highlights:

- Three new coordination polymers were synthesized and characterized.
- The mixed ligands strategy of 5-hydroxy isophthalic acid and 1,3-bis(imidazol-1-ylmethyl)benzene ligands were introduced to design coordination polymers.
- Metal ions coordination preferences play important roles in determining the three coordination polymers.
- The structural diversity, magnetic and photoluminescence properties were also discussed.

Pictogram: The coordination preferences of different metal ions in synthetic procedures of the three mixed ligands based coordination polymers.





ELSEVIER

Contents lists available at [SciVerse ScienceDirect](http://www.sciencedirect.com)**Inorganic Chimica Acta**journal homepage: www.elsevier.com/locate/ica

Metal-Dependent Structural Variations Based on Mixed Ligands of 5-Hydroxy Isophthalic Acid and 1,3-Bis(imidazol-1-ylmethyl)benzene: Solvothermal Syntheses, Structural Characterizations, Luminescence and Magnetic Properties

Xiutang Zhang,^{*a,b} Liming Fan,^{a,b} Weiliu Fan,^b and Xian Zhao^{*b}

^a Advanced Material Institute of Research, College of Chemistry and Chemical Engineering, Qilu Normal University, Jinan, 250013, China. E-mail: xiutangzhang@163.com;

^b State Key Laboratory of Crystal Materials, Shandong University, Jinan 250100, China. E-mail: xianzhao@sdu.edu.cn.

Keywords: 5-Hydroxy isophthalic acid, 1,3-Bis(imidazol-1-ylmethyl)benzene, Coordination preference, Luminescent property, Magnetic property

ABSTRACT

Three 5-hydroxy isophthalic acid (H₂OIP) based coordination polymers, namely, {[Cu(OIP)(bimb)]•H₂O}_n (**1**), {[Co₂(OIP)₂(bimb)₂]•H₂O}_n (**2**), and [Zn(OIP)(bimb)]_n (**3**) were synthesized under hydrothermal conditions in the presence of bis(imidazole) bridging linkers (bimb = 1,3-bis(1H-imidazol-4-yl)benzene) (bimb)). Their structures have been determined by single-crystal X-ray diffraction analysis and further characterized by elemental analysis, IR spectra, powder X-ray diffraction (PXRD), and thermogravimetric (TG) analysis. Complex **1** displays a 3D ABAB packing supramolecular structure with 4-connected 2D wave sql sheet. Complex **2** possesses a 3D 5-connected bnn net based on [Co₂(COO)₂] secondary building unit (SBU) with a Schläfli symbol of (4⁶•6⁴). Complex **3** features a 2D flat sql net with Zn ions as 4-connected nodes. Moreover, the magnetic property of complex **2** and the solid state luminescence of complex **3** have been investigated.



ELSEVIER

Contents lists available at SciVerse ScienceDirect

Inorganic Chimica Acta

journal homepage: www.elsevier.com/locate/ica

Metal-Dependent Structural Variations Based on Mixed Ligands of 5-Hydroxy Isophthalic Acid and 1,3-Bis(imidazol-1-ylmethyl)benzene: Solvothermal Syntheses, Structural Characterizations, Luminescence and Magnetic Properties

Xiutang Zhang,^{*a,b} Liming Fan,^{a,b} Weiliu Fan,^b Xian Zhao^{*b}

^a Advanced Material Institute of Research, College of Chemistry and Chemical Engineering, Qilu Normal University, Jinan, 250013, China.

^b State Key Laboratory of Crystal Materials, Shandong University, Jinan 250100, China.

ARTICLE INFO

Article history:

Received 01 January 2015

Received in revised form

01 January 2015

Accepted 01 January 2015

Available online 01 January 2015

Keywords:

5-Hydroxy isophthalic acid

1,3-bis(1H-imidazol-4-yl)benzene

Coordination preference

Luminescent property

Magnetic property

ABSTRACT: Three 5-hydroxy isophthalic acid (H₂OIP) based coordination polymers, namely, {[Cu(OIP)(bimb)]•H₂O}_n (**1**), {[Co₂(OIP)₂(bimb)₂]•H₂O}_n (**2**), and [Zn(OIP)(bimb)]_n (**3**) were synthesized under hydrothermal conditions in the presence of bis(imidazole) bridging linkers (bimb = 1,3-bis(1H-imidazol-4-yl)benzene (bimb)). Their structures have been determined by single-crystal X-ray diffraction analysis and further characterized by elemental analysis, IR spectra, powder X-ray diffraction (PXRD), and thermogravimetric (TG) analysis. Complex **1** displays a 3D ABAB packing supramolecular structure with 4-connected 2D wave **sql** sheet. Complex **2** possesses a 3D 5-connected **bnn** net based on [Co₂(COO)₂] secondary building unit (SBU) with a Schläfli symbol of (4⁶•6⁴). Complex **3** features a 2D flat **sql** net with Zn ions as 4-connected nodes. Moreover, the magnetic property of complex **2** and the solid state luminescence of complex **3** have been investigated.

1. Introduction

Functional coordination polymers (CPs), a class of novel solid materials, have attracted thousands of coordination chemists and engineers for their interesting structures as well as potential applications in gas separation and storage, catalysis, magnetism, optical properties, and microelectronics sensing [1–4]. The architectures and functions of these materials can be tailored by altering factors such as the metal cations, solvent media, templating agent, pH, counteranion, and the chemical structure of organic ligands [5–7]. Strategically designed or select featured organic ligands according to their length, rigidity, coordination modes, and functional groups or substituents were proved to be an efficient route for achieving the expected CPs [8].

However, the controllable synthesis of prospective networks is still a far-reaching challenge since such

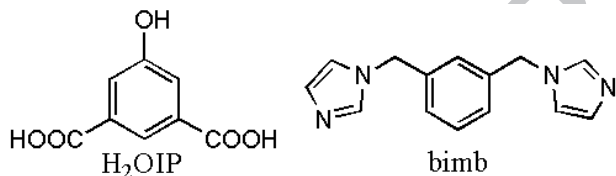
materials are always dependent on many uncertain factors, such as the coordination geometry preferred by the metal, solvent systems, templates, pH values, counteranions, and the chemical structures of the selected ligands [7–12]. Among these factors, the rational selection of the characteristic ligand proved to be one efficient route for the construction of versatile CPs. Generally, the length, rigidity, coordination modes, and functional groups or substituents of polycarboxylate ligands have consequential effects on the final structures of CPs [13]. Moreover, a recent study on coordination assemblies using (bis)imidazole linkers as ancillary ligands provided a reliable strategy for obtaining new topological prototypes of coordination nets [14]. The ancillary ligands have a great effect on the coordination modes of the host polycarboxylate aromatic acid and the final packing structures. With the length of the ancillary ligands increasing, the longer separation of neighboring central ions makes the host aromatic polycarboxylate ligand adopt more “open” coordination modes and the overall structure a higher degree of interpenetration. The greater

*Corresponding author.

E-mail address: xiutangzhang@163.com (X. Zhang); xianzhao@sdu.edu.cn (X. Zhao).

flexibility of ancillary ligands could make the final structure more twisted and complicated [15]. Thus, CPs can be assembled from predetermined organic building blocks through judicious selection of ligands and careful control of reaction conditions. To the best of our knowledge, CPs based on 5-hydroxy isophthalic acid (H₂OIP) in the presence of 1,3-bis(1H-imidazol-4-yl)benzene (bimb) have never been documented to date [16-19]. On the other hands, the mixed-ligand strategy has been proved to be efficient in the assembly of numerous CPs [20-27]. Compared to the ordinary cheating N-donors, such as the 2,2-bipyridine (bpy), and phenanthroline (phen), it is no doubt that the 1,3-bis(1H-imidazol-4-yl)benzene (bimb) could be employed to construct high-dimension CPs more easily due to that the flexible backbones of the bimb can adjust itself to coordinate with metal ions by twisting, rotating, folding, and so on [28-30].

Thus, these considerations inspired us to explore new coordination frameworks with 5-hydroxy isophthalic acid (H₂OIP) and 1,3-bis(1H-imidazol-4-yl)benzene (bimb), shown in Scheme 1). Herein, we reported the syntheses and characterizations of three new coordination polymers, {[Cu(OIP)(bimb)]·H₂O}_n (**1**), {[Co₂(OIP)₂(bimb)₂]·H₂O}_n (**2**), and [Zn(OIP)(bimb)]_n (**3**), which exhibit a systematic variation of architectures from 2D flat **sql** net, 2D wave **sql** net, to 3D (4⁶.6⁴)-**bnn** net. Structural comparisons indicated that the metal ions are crucial factors for in determining the structural diversity of coordination polymers. In addition, the magnetic property of complex **2** and the solid state luminescence of complex **3** have been investigated.



Scheme 1. The organic ligands in the assembly of titled complexes.

2. Experimental

2.1. Materials and Methods

All the chemical reagents were purchased from Jinan Henghua Sci. & Tec. Co. Ltd. without further purification. Elemental analyses of C, N, and H were performed on an EA1110 CHNS-0 CE elemental analyzer. IR (KBr pellet) spectra were recorded on a Nicolet Magna 750FT-IR spectrometer. Thermogravimetric measurements were carried out in a nitrogen stream using a Netzsch STA449C apparatus with a heating rate of 10 °C min⁻¹. X-Ray powder diffraction (XRPD) was carried out on a RIGAKU DMAX2500 apparatus. Fluorescent data were collected on an Edinburgh FLS920 TCSPC system. Fluorescent data were collected on an Edinburgh FLS920 TCSPC system. The variable-temperature magnetic susceptibility measurements were performed on the Quantum Design SQUID MPMS XL-7 instruments in the temperature range of 2-300 K under a field of 1000 Oe.

2.2. Syntheses

2.2.1. Preparation of {[Cu(OIP)(bimb)]·H₂O}_n (**1**)

A mixture of H₂OIP (0.30 mmol, 0.055 g), bib (0.30 mmol, 0.071 g), CuSO₄·5H₂O (0.30 mmol, 0.075 g), NaOH (0.30 mmol, 0.012 g), 6 mL H₂O and 3 mL CH₃CN was sealed in a 25 mL Teflon-lined stainless steel vessel, which was heated to 150 °C for 3 days and then cooled to 25 °C at a rate of 10 °C h⁻¹. Blue block crystals of **1** were obtained with the yield of 47 % (based on Cu). Anal. (%) calcd. for C₂₂H₂₀CuN₄O₆: C, 52.85; H, 4.03; N, 11.21. Found: C, 52.71; H, 4.26; N, 10.98. IR (KBr pellet, cm⁻¹): 3486 (m), 3096 (m), 1683 (s), 1569 (s), 1421 (vs), 1121 (m), 897 (w), 838 (m), 753 (w).

2.2.2. Preparation of {[Co₂(OIP)₂(bimb)₂]·H₂O}_n (**2**)

The same synthetic procedure as for **1** was used except that CuSO₄·5H₂O was replaced by CoSO₄·7H₂O, giving purple block crystals. The precipitate that formed was collected by filtration, and dried at room temperature to give **2** in 53 % yield based on Co. Anal. (%) calcd. for C₄₄H₃₈Co₂N₈O₁₁: C, 54.33; H, 3.94; N, 11.52. Found: C, 53.96; H, 4.10; N, 11.38. IR (KBr pellet, cm⁻¹): 3451 (m), 3121 (w), 1748 (m), 1623 (vs), 1461 (s), 1276 (w), 1147 (s), 857 (m), 776 (m).

2.2.3. Preparation of [Zn(OIP)(bimb)]_n (**3**)

The same synthetic procedure as for **1** was used except that CuSO₄·5H₂O was replaced by ZnSO₄·7H₂O, giving colourless block crystals. The precipitate that formed was collected by filtration, and dried at room temperature to give **3** in 61 % yield based on Zn. Anal. (%) calcd. for C₁₁H₉N₂O_{2.5}Zn_{0.5}: C, 54.62; H, 3.75; N, 11.58. Found: C, 54.45; H, 3.89; N, 11.36. IR (KBr pellet, cm⁻¹): 3457 (m), 3130 (w), 1787 (w), 1693 (vs), 1548 (s), 1486 (s), 1321 (m), 996 (m), 913 (m), 756 (m).

2.3. X-ray crystallography

Single crystals of the complexes **1-3** with appropriate dimensions were chosen under an optical microscope and quickly coated with high vacuum grease (Dow Corning Corporation) before being mounted on a glass fiber for data collection. Intensity data collection was carried out on a Siemens SMART diffractometer equipped with a CCD detector using MoK α monochromatized radiation ($\lambda = 0.71073 \text{ \AA}$) at 296(2) K. The absorption correction was based on multiple and symmetry-equivalent reflections in the data set using the SADABS program. The structures were solved by direct methods and refined by full-matrix least-squares using the SHELXTL package [31]. Anisotropic thermal parameters were applied to all non-hydrogen atoms. And all hydrogen atoms attached to C and N atoms were placed geometrically [32]. Crystallographic data for complexes **1-3** are given in Table 1. Selected bond lengths and angles for **1-3** are listed in Table S1.

Table 1 Crystal data for **1-3**

Complex	1	2	3
Formula	C ₂₂ H ₂₀ CuN ₄ O ₆	C ₄₄ H ₃₈ Co ₂ N ₈ O ₁₁	C ₁₁ H ₉ N ₂ O _{2.5} Zn _{0.5}
<i>M_r</i>	499.96	972.68	241.89
Crystal system	Monoclinic	Monoclinic	Monoclinic
Space group	<i>P2₁/n</i>	<i>P2₁/n</i>	<i>P2₁/n</i>
<i>a</i> (Å)	10.1050(11)	9.9842(4)	10.8851(4)
<i>b</i> (Å)	19.2546(19)	34.3888(17)	16.5714(6)

<i>c</i> (Å)	11.1318(11)	11.8547(5)	12.0802(4)
β (°)	91.590(3)	99.7390(10)	112.7180(10)
<i>V</i> (Å ³)	2165.1(4)	4011.6(3)	2009.98(12)
<i>Z</i>	4	4	8
ρ (g cm ⁻³)	1.534	1.611	1.599
μ (mm ⁻¹)	1.057	0.904	1.267
<i>T</i> (K)	296(2)	296(2)	296(2)
<i>F</i> (000)	1028	2000	992
<i>R</i> _{int}	0.0643	0.0714	0.0469
<i>R</i> [<i>I</i> > 2 σ (<i>I</i>)] ^a	<i>R</i> ₁ = 0.0418 <i>wR</i> ₂ = 0.0944	<i>R</i> ₁ = 0.0407 <i>wR</i> ₂ = 0.0907	<i>R</i> ₁ = 0.0285 <i>wR</i> ₂ = 0.0574
<i>R</i> (all data) ^a	<i>R</i> ₁ = 0.0646 <i>wR</i> ₂ = 0.1057	<i>R</i> ₁ = 0.0693 <i>wR</i> ₂ = 0.1033	<i>R</i> ₁ = 0.0352 <i>wR</i> ₂ = 0.0608
Gof	1.001	0.999	0.999
CCDC number	1402562	1402563	1402625

^a*R*₁ = $\sum |F_o| - |F_c| / \sum |F_o|$, *wR*₂ = $[\sum w(F_o^2 - F_c^2)^2] / \sum w(F_o^2)^2$

3. Result and discussion

3.1. Descriptions of crystal structures

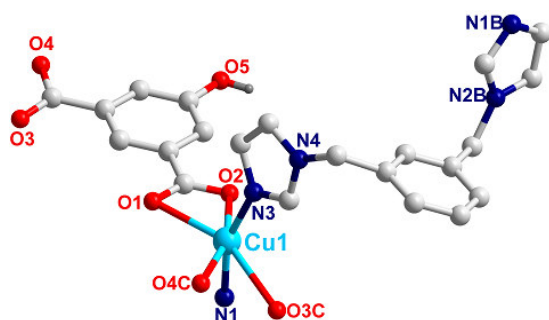


Figure 1. The asymmetric unit of complex **1** (Symmetry codes: B: *x*, *y*, 1+*z*; C: 1/2-*x*, -1/2+*y*, 3/2-*z*).

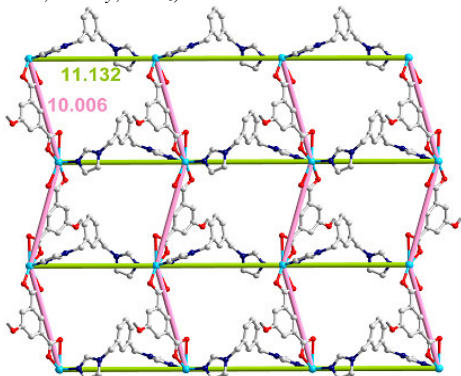


Figure 2. The 2D flat [Cu(OIP)(bimb)] sheet containing the 1D [Cu(bimb)]_{*n*} and 1D [Cu(OIP)]_{*n*} chains.

3.1.1. {[Cu(OIP)(bimb)]·H₂O}_{*n*} (1)

The single-crystal X-ray diffraction analysis reveals that complex **1** crystallizes in the monoclinic system, *P*2₁/*n* space group, and the asymmetric unit of **1** consists of one Cu^{II} ion, one OIP²⁻ ligand, one bimb ligand, and one lattice water molecule. As shown in Fig. 1a, the Cu^{II} center locates in a distorted octahedral geometry, coordinated by four O atoms from two different OIP²⁻ ligands and two N atoms from two distinct bimb ligands, and the angles around it fall in the range of 89.38(10)–160.70(8)°.

The OIP²⁻ ligand act as bridging linker to bind two Cu^{II} ions through two ($\kappa^1-\kappa^1$) cheating carboxyl groups, leaving a 1D flat [Cu(OIP)]_{*n*} chains with the neighboring Cu^{II} distances being 10.006 Å (Fig. S1). Along the other direction, the bimb bridged

the Cu^{II} ions, forming a 1D straight [Cu(bimb)]_{*n*} chain with the adjacent Cu^{II} ions distance is 11.132 Å (Fig. S2). Sharing with the Cu^{II} centers, a 2D sheet was constructed (Fig. 2). The neighboring sheets packed with each other with ABAB arrangement through the hydrogen bonds interaction [O5–H5...O3ⁱ = 2.600 Å, Symmetry code: i: *x*+1/2, -*y*+3/2, *z*+1/2.], finally given a 3D supramolecular structure (Fig. 3). Besides, hydrogen bonds [O1w–H2w...O5ⁱⁱ = 2.854 Å, O1w–H1w...O4ⁱⁱⁱ = 3.021 Å, Symmetry codes: ii: *x*-1/2, -*y*+3/2, *z*-1/2; iii: -*x*+3/2, *y*-1/2, -*z*+3/2.] between lattice water molecules and the sheets also play important roles in maintaining the stability of the supramolecular architecture.

From the viewpoint of topology [33], the final structure of **1** can be defined as **sql** sheet. If we take the hydrogen bonds into consideration, the 3D supramolecular frameworks can be simplified to be a 6-connected **pcu** net (Fig. 4).

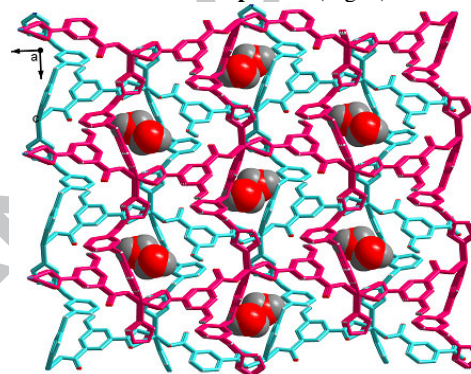


Figure 3. The 3D supramolecular structure of complex **1** by ABAB sheets packing.

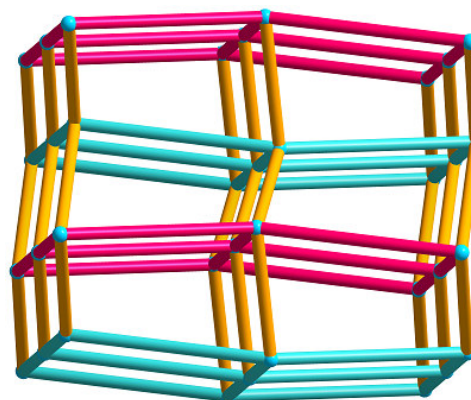


Figure 4. The **pcu** topology for the 3D supramolecular structure of complex **1**.

3.1.2. {[Co₂(OIP)₂(bimb)₂]·H₂O}_{*n*} (2)

Single-crystal X-ray diffraction analysis reveals that complex **2** crystallizes in the monoclinic system, *P*2₁/*n* space group, and the asymmetric unit of **2** consists of two Co^{II} ions, two OIP²⁻ ligands, two bimb ligands, and one lattice water molecule. As illustrated in Fig. 5, Co(1) is located at a general center with a trigonal bipyramidal geometry surrounded by three O atoms from three different OIP²⁻ ligands occupying the basal positions [Co(1)–O(1) = 2.001(2) Å, Co(1)–O(7) = 2.049(2) Å, and Co(1)–O(9)D = 2.011(2) Å] and two N atoms forming the apical positions [Co(1)–N(1) = 2.119(3) Å, and Co(1)–N(7) = 2.134(3) Å]. Co(2) is located in a similar

[CoN₂O₃] trigonal bipyramidal geometry, coordinated by three O atoms from three different OIP²⁻ ligands [Co(2)–O(2) = 2.0401(19) Å, Co(2)–O(3)D = 2.065(2) Å, and Co(2)–O(8)D = 2.017(2) Å], two N atoms from two bimb ligands [Co(2)–N(2) = 2.092(3) Å, and Co(2)–N(4) = 2.127(3) Å], respectively.

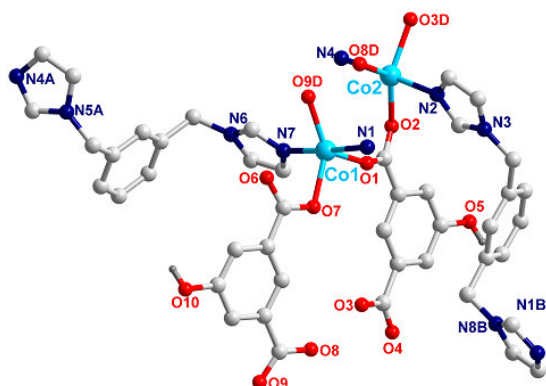


Figure 5. The asymmetric unit of complex **2** (Symmetry codes: A: $1-x, -y, 2-z$; B: $1/2+x, 1/2-y, -1/2+z$; D: $-x+1, y, z$).

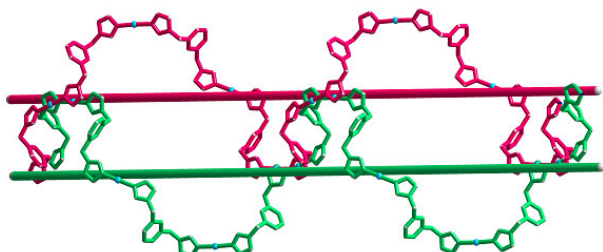


Figure 6. The unprecedented 1D right- and left-handed [Co(bimb)]_n helix chains.

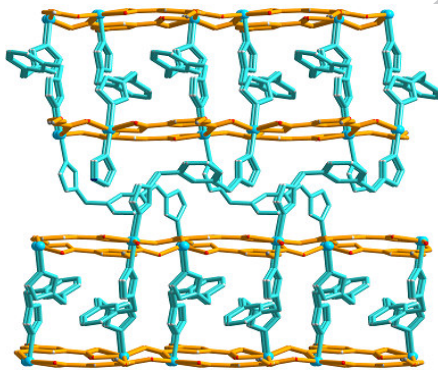


Figure 7. The 3D frameworks of complex **2**.

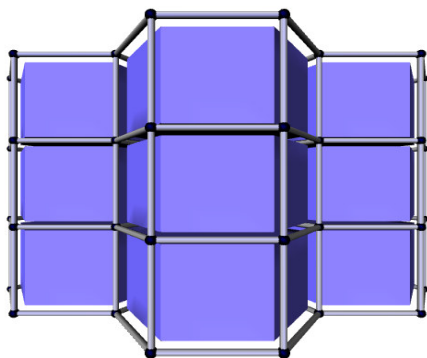


Figure 8. The tiling featured **bnn** net for complex **2**.

The OIP²⁻ ligands link Co^{II} ions to form a 1D [Co(OIP)]_n ladder chains with the binuclear [Co₂(COO)₂]_n SBUs (Fig. S3).

It is noteworthy that the unprecedented [Co(bimb)]_n chains with right- and left-handed chiral characteristics were built from the bimb connecting the Co^{II} ions, with the Co^{II}–Co distances are 12.861 and 12.745 Å, respectively (Fig. 6). Then those chains hinged together, further given a 3D frameworks (Fig. 7). At the sight of topology, the final structure of **2** can be defined as a 5-connected **bnn** net with the Schläfli symbol of (4⁶.6⁴) by denoting the [Co₂(COO)₂]_n SBUs to 5-connected nodes, and all the organic ligands as linkers, respectively (Fig. S4 and Fig. 8).

3.1.3. [Zn(OIP)(bimb)]_n (**3**)

The single-crystal X-ray diffraction analysis reveals that compound **3** crystallizes in the monoclinic system, *P*₂/*n* space group, and the asymmetric unit of **3** consists of one Zn^{II} ions, one OIP²⁻ ligand, and one bimb ligand. As shown in Fig. 9, each Zn^{II} ion is surrounded by two O atoms [Zn(1)–O(1) = 1.9728(15) Å and Zn(1)–O(3)D = 1.9750(16) Å] from two individual OIP²⁻ ligands and two N atoms [Zn(1)–N(1) = 2.031(2) Å and Zn(1)–N(3) = 2.0178(19) Å] from bimb ligands, showing a tetrahedral geometry. And the angles around the Zn^{II} ions fall in the range of 94.32(7)–120.36(8)^o, respectively.

Similar with that in complex **1**, a 1D flat [Zn(OIP)]_n chain was constructed from the OIP²⁻ ligands linked with Zn^{II} ions through the monodentate carboxyl groups (Fig. S5). And the OIP²⁻ ligand separated Zn^{II}–Zn^{II} distance is 9.615 Å. Moreover, the bridging bimb ligands coordinated with the Zn^{II} ions, forming a 1D wave [Zn(bimb)]_n chain (Fig. S6). And then the two kinds of chains joined together by sharing the metal centres, finally given a 2D bilayer (Fig. 10). The adjacent sheets were further expanded to a 3D supramolecular structure through the conjugation effect (Fig. 11). In the view of topology, the 3D supramolecular framework can be simplified the 6-connected **pcu** net with (4¹².6³) topological symbol (Fig. 12).

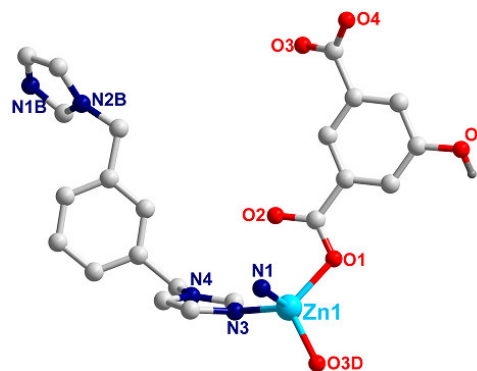


Figure 9. The asymmetric unit of complex **3** (Symmetry codes: B: $3/2-x, -1/2+y, -1/2-z$; D: $-1/2+x, 1/2-y, 1/2+z$).

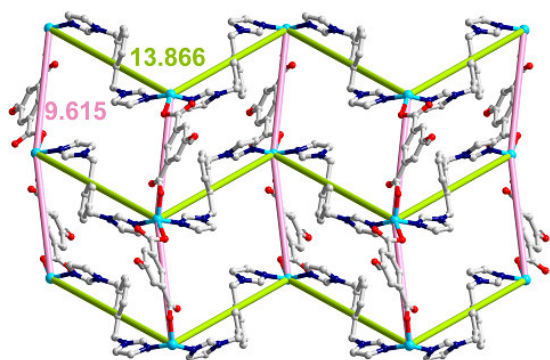


Figure 10. The 2D wave [Zn(OIP)(bimb)] sheet containing the 1D [Zn(bimb)]_n and 1D [Zn(OIP)]_n chains.

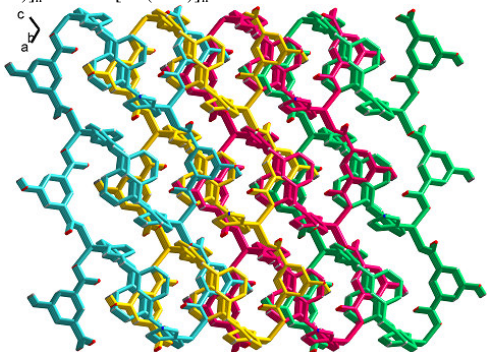


Figure 11. The 3D packing supramolecular structures of complex 3.

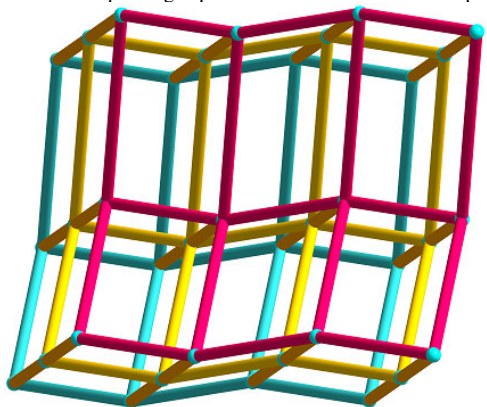


Figure 12. The hydrogen bonds based **pcu** net for the 3D supramolecular structure of complex 3.

3.2. Coordination preferences and structure diversity

Complexes **1-3** were synthesized under similar reaction condition except the use of different transition metal ions (Cu^{II} , Co^{II} , and Zn^{II}), their coordination structures with different dimensionalities and diversity architectures can be mainly ascribed to the different coordination preferences of metal ions. Indeed, Cu^{II} ions trend to be cheated by two cheating carboxyl groups from OIP^{2-} ligands, forming a 1D flat $[\text{Cu}(\text{OIP})]_n$ chain. And each bimb bridged two neighbouring Cu^{II} ions, constructed a 1D straight $[\text{Cu}(\text{bimb})]_n$ chain. The two kinds of chains joined together, finally given a 2D **sql** sheet. For complex **2**, the Co^{II} ions tend to form dinuclear units by two $\mu_2\text{-}\eta^1, \eta^1$ -bridging carboxyl groups, and the dinuclear units are further interlinked by OIP^{2-} ligands to form a 1D ladder chain. Besides, the bimb linked the Co^{II} ions, giving an unprecedented $[\text{Co}(\text{bimb})]_n$ chain with right- and left-

handed helix characteristics in **2**. For complex **3**, the Zn^{II} ion has a preference to locate in a tetrahedral geometry, and hence the Zn^{II} ions linked by OIP^{2-} ligands to form a 1D flat $[\text{Zn}(\text{OIP})]_n$ chain. The bimb ligands connected with Zn^{II} ions, formed a 1D $[\text{Zn}(\text{bimb})]_n$ wave chain. Then the 1D $[\text{Zn}(\text{OIP})]_n$ chains and $[\text{Zn}(\text{bimb})]_n$ wave chains further expanded the structures to a 2D wave sheet. The comparison study reveals that the metal ions play important roles in determining the structural diversity of coordination polymers. And the mixed ligands strategy expanded the field of functional coordination polymers.

3.3. Powder X-ray diffraction (PXRD) and IR Spectra

In order to check the phase purity of these complexes, the PXRD patterns of title complexes were checked at room temperature. As shown in Fig. S7, the peak positions of the simulated and experimental PXRD patterns are in agreement with each other, demonstrating the good phase purity of the complexes. The dissimilarities in intensity may be due to the preferred orientation of the crystalline powder samples.

The main features of IR spectra for complexes **1**, **2** and **3** concerned the carboxyl groups of H_2OIP ligand. As can be seen in Fig. S8, no strong absorption peaks around 1800 cm^{-1} for $-\text{COOH}$ are observed, which implies that carboxyl groups of organic moieties in the title complexes are completely deprotonated. The strong peaks at 1569 and 1421 cm^{-1} for **1**, 1623 and 1461 cm^{-1} for **2**, and 1693 , and 1486 cm^{-1} for **3** may be attributed to the asymmetric and symmetric vibrations of carboxyl groups. The ($\nu_{\text{as}}-\nu_{\text{s}}$) values (148 cm^{-1} for **1**, 164 cm^{-1} for **2**, and 207 cm^{-1} for **3**) are attributed to the diverse carboxylate coordination modes, which are in accordance with the spectroscopic criteria on determining the modes of the carboxylate binding ($\Delta(\text{chelating}) < \Delta(\text{bridging}) < \Delta(\text{ionic}) < \Delta(\text{monodentate})$) [34].

3.4. Thermal analysis

The experiments were performed on samples consisting of numerous single crystals under N_2 atmosphere with a heating rate of $10\text{ }^\circ\text{C min}^{-1}$, as shown in Fig. S8. For complex **1**, a weight loss of 3.8 % was observed around $100\text{ }^\circ\text{C}$, which corresponds to the loss of the lattice water molecules (calcd 3.6 %), and then the network began to decompose with the loss of two organic ligands at about $335\text{ }^\circ\text{C}$, with the residual weight is ca. 16.2 % (Calcd. for CuO : 15.9 %). Similar with complex **1**, complex **2** shows a weight loss of 1.91 % in the temperature range of $90\text{-}120\text{ }^\circ\text{C}$ corresponding to the release of the free water molecules (calcd 1.86 %) and the decomposition of the residue occurred at $360\text{ }^\circ\text{C}$. The residual weight is ca. 19.6 % (Calcd. for CoO : 18.7 %). For complex **3**, the network can be exist stably until the temperature up to $280\text{ }^\circ\text{C}$, and then the subsequent significant weight losses occur after the onset temperature with the residual weight is ca. 17.3 % (Calcd. for ZnO : 16.7 %). It is obvious that the thermal stability of **2** is higher than that of **1** and **3**.

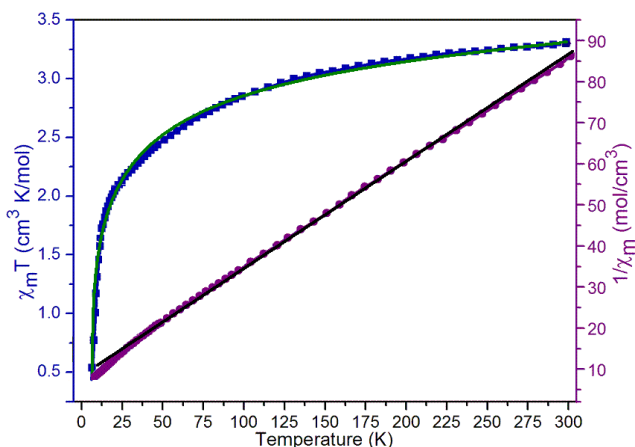


Figure 13. The temperature dependence of magnetic susceptibility of **2** under a static field of 1000 Oe.

3.5. Magnetic property of complex **2**.

As shown in Fig. 13, the $\chi_M T$ values for **2** at room temperature are $3.39 \text{ cm}^3 \text{ K mol}^{-1}$ (Fig. 13), which is smaller than that for two isolated Co^{II} cations ($3.75 \text{ cm}^3 \text{ K mol}^{-1}$), which can be attributed to the contribution to the susceptibility from orbital angular momentum at higher temperatures. With the temperature decreasing, the $\chi_M T$ value decreases continuously to $0.47 \text{ cm}^3 \text{ K mol}^{-1}$ at 2 K. And the temperature dependence χ_M followed the Curie-Weiss law $\chi_M = C/(T - \theta)$ with $C = 3.96 \text{ cm}^3 \text{ K mol}^{-1}$, $\theta = -39.68 \text{ K}$. The negative value of θ indicates the presence of an antiferromagnetic interaction between the nearest Co^{II} ions. The fitting result is comparable with those reported Co^{II} dinuclear coordination polymers [35].

3.6. Photoluminescent property of complex **3**

The photoluminescence spectra of the two organic ligands and complex **3** were examined in the solid state at room temperature and given in Fig. 14. Intense emission band of pure free H_2OIP and *bimb* ligands have been observed at 380 nm ($\lambda_{\text{ex}} = 280 \text{ nm}$), and 338 nm ($\lambda_{\text{ex}} = 290 \text{ nm}$), respectively, which can be presumed that the peak originate from the $\pi^* \rightarrow n$ or $\pi^* \rightarrow \pi$ transitions [36, 37]. It can be observed that intense emissions occur at 358 nm ($\lambda_{\text{ex}} = 323 \text{ nm}$) for **3**. The emission peak of complex **3** is red shift by about 20 nm compared to the *bimb* ligand, but it is also blue shift by about 22 nm compared to the free H_2OIP ligand, respectively. The emissions of complex **3** is tentatively assigned to the intraligand transition due to their similarity to ligands, since Zn^{II} ion is difficult to oxidize or to reduce due to its d^{10} configuration [38].

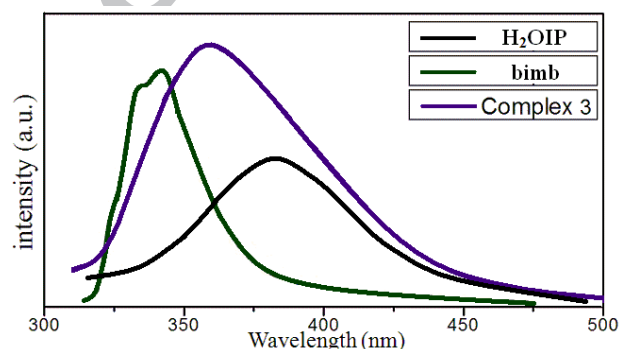


Figure 14. Emission spectra of two organic ligands and complex **3** in the solid state at room temperature.

4. Conclusions

In summary, three multi-dimensional MOFs were isolated from the hydrothermal reactions by the employment of 5-hydroxy isophthalic acid (H_2OIP) and 1,3-bis(1H-imidazol-4-yl)benzene (*bimb*). Complexes **1–3** displayed appealing structural features from 2D layers to 3D frameworks. Structural analyses reveals that H_2OIP is an effective ligand with rich coordination modes, which is useful to better understand the synthon selectivity in multifunctional crystal structures. In addition, the employment of the *bimb* bridging ligands during the assembly of the metal–polycarboxylate system often leads to structural changes and affords new frameworks.

Acknowledgements

The work was supported by financial support from the Natural Science Foundation of China (Grant Nos. 21101097, 21451001), key discipline and innovation team of Qilu Normal University.

Appendix A. Supporting information

Supplementary data associated with this article can be found in the online version at <http://dx.doi.org/10.1016/j.ica.2015.xx.xxx>.

References

- [1] A. Proust, B. Matt, R. Villanneau, G. Guillemot, P. Gouzerh, G. Izzet, *Chem. Soc. Rev.* 41 (2012) 7605.
- [2] H.C. Zhou, J.R. Long, O.M. Yaghi, *Chem. Rev.* 112 (2012) 673.
- [3] X.T. Zhang, D. Sun, B. Li, L.M. Fan, B. Li, P.H. Wei, *Cryst. Growth Des.* 12 (2012) 3845.
- [4] C.J. Sumby, *Coord. Chem. Rev.* 255 (2011) 1937.
- [5] D.S. Li, Y.P. Wu, J. Zhao, J. Zhang, J.Y. Lu, *Coord. Chem. Rev.* 261 (2014) 1.
- [6] L.M. Fan, X.T. Zhang, D.C. Li, D. Sun, W. Zhang, J.M. Dou, *Cryst. Eng. Comm.* 15 (2013) 349.
- [7] F.T. Xie, H.Y. Bie, L.M. Duan, G.H. Li, X. Zhang, J.Q. Xu, *J. Solid State Chem.* 178 (2005), 2858.
- [8] L.L. Liu, C.X. Yu, Y.R. Li, J.J. Han, F.J. Ma, L.F. Ma, *Cryst. Eng. Comm.* 17 (2015) 653.
- [9] X.T. Zhang, L.M. Fan, Z. Sun, W. Zhang, D.C. Li, J.M. Dou, L. Han, *Cryst. Growth Des.* 13 (2013) 792.
- [10] M. Du, X.J. Zhao, J.H. Guo, S.R. Batten, *Chem. Commun.* (2005) 4836.
- [11] F. Guo, F. Wang, H. Yang, X.L. Zhang, J. Zhang, *Inorg. Chem.* 51 (2012) 9677.
- [12] X. Zhang, L. Fan, W. Fan, B. Li, X. Zhao, *Cryst. Eng. Comm.* 17 (2015) 6681.
- [13] J. Jin, D. Li, L. Li, X. Han, S. Cong, Y. Chi, S. Niu, *Inorg. Chim. Acta* 379 (2011), 44.
- [14] L.L. Liu, C.X. Yu, F.J. Ma, Y.R. Li, J.J. Han, L. Lin, J.F. Ma, *Dalton Trans.* 44 (2015) 1636.
- [15] F. Guo, *Inorg. Chim. Acta* 399 (2013), 79.
- [16] Y. Xu, D. Yuan, B. Wu, L. Han, M. Wu, F. Jiang and M. Hong, *Cryst. Growth Des.* 6 (2006) 1168.
- [17] X.T. Zhang, L.M. Fan, X. Zhao, D. Sun, D.C. Li, J.M. Dou, *Cryst. Eng. Comm.* 14 (2012) 2053.
- [18] Y.X. Sun, W.Y. Sun, *Cryst. Eng. Comm.* 17 (2015) 4045.
- [19] J. Bai, H.-L. Zhou, P.-Q. Liao, W.-X. Zhang, X.-M. Chen, *Cryst. Eng. Comm.* 17 (2015) 4462.
- [20] L. Fan, X. Zhang, W. Zhang, Y. Ding, W. Fan, L. Sun, X. Zhao, *Cryst. Eng. Comm.* 16 (2014) 2144.
- [21] G. Xu, F. Guo, *Inorg. Chem. Commun.* 27 (2013) 146.
- [22] X. Zhang, L. Fan, W. Zhang, W. Fan, L. Sun, X. Zhao,

- Cryst. Eng. Comm. 16 (2014) 3203.
- [23] L. Fan, X. Zhang, W. Zhang, Y. Ding, W. Fan, L. Sun, Y. Pang, X. Zhao, Dalton Trans. 43 (2014) 6701
- [24] L. Fan, W. Fan, W. Song, L. Sun, X. Zhao, X. Zhang, Dalton Trans. 43 (2014) 15979.
- [25] L. Fan, Y. Gao, G. Liu, W. Fan, W. Song, L. Sun, X. Zhao, X. Zhang, Cryst. Eng. Comm. 16 (2014) 7649.
- [26] L. Fan, W. Fan, B. Li, X. Liu, X. Zhao, X. Zhang, Dalton Trans. 44 (2015) 2380
- [27] M. Dai, X.-R. Su, X. Wang, B. Wu, Z.-G. Ren, X. Zhou, J.-P. Lang, Cryst. Growth Des. 14 (2014) 240.
- [28] Z.-H. Yan, L.-L. Han, Y.-Q. Zhao, X.-Y. Li, X.-P. Wang, L., D. Sun, Cryst. Eng. Comm. 16 (2014) 8747.
- [29] J.-J. Wang, L. Tang, M.-L. Zhang, L.-J. Gao, Y.-X. Ren, X.-Y. Hou, F. Fu, J. Mol. Struct. 1085 (2015) 215.
- [30] L. Fan, W. Fan, B. Li, X. Zhao, X. Zhang, RSC Adv. 5 (2015) 39854.
- [31] G.M. Sheldrick, SHELXS-97, Program for solution of crystal structures, University of Göttingen, Germany, 1997.
- [32] G. M. Sheldrick, SHELXL-97, Program for refinement of crystal structures, University of Göttingen, Germany, 1997.
- [33] V.A. Blatov, M. O'Keeffe, D.M. Proserpio, Cryst. Eng. Comm. 12 (2010) 44.
- [34] L.M. Fan, X.T. Zhang, Z. Sun, W. Zhang, Y.S. Ding, W.L. Fan, L.M. Sun, X. Zhao, H. Lei, Cryst. Growth Des. 13 (2013) 2462.
- [35] M.L. Han, Y.P. Duan, D.S. Li, H.B. Wang, J. Zhao, Y.Y. Wang, Dalton Trans. 43 (2014) 15450
- [36] K. Jiang, L.-F. Ma, X.-Y. Sun, L.-Y. Wang, Cryst. Eng. Comm. 13 (2011) 330.
- [37] B.-F. Huang, T. Sun, Z. Sharifzadeh, M.-Y. Lv, H.-P. Xiao, X.-H. Li, A. Morsali, Inorg. Chim. Acta 405 (2013) 83.
- [38] T. Cao, Y. Peng, T. Liu, S. Wang, J. Dou, Y. Li, C. Zhou, D. Li, J. Bai, Cryst. Eng. Comm. 16 (2014) 10658.